DESIGN, DEVELOPMENT AND TESTING OF A SCAN AND FOCUS MECHANISM FOR THE SPICE INSTRUMENT

W Holmes [(1)], G Munro [(1)], O Poyntz-Wright [(1)]

[(1)] *ESR Technology (a part of the Hyder Consulting Group), 202 Cavendish Place, Birchwood Park, Warrington, WA3 6WU, UK. Email: william.holmes@esrtechnology.com*

ABSTRACT

The Scan and Focus Mechanism (SFM) is one of four mechanisms within the SPICE (SPectral Imaging of the Coronal Environment) instrument and is used to provide scan rotation and linear focus adjustment for the instrument's primary mirror. The design of the mechanism is based around the use of two titanium flexure based stages which provide compliance in the required degrees of freedom and high stiffness and stability in others. This paper presents an overview of the design and qualification activities carried out to date and discusses lessons learned.

1. INTRODUCTION

The Scan and Focus Mechanism (SFM) is one of four mechanisms that form the SPICE (SPectral Imaging of the Coronal Environment) instrument. SPICE is a high resolution imaging spectrometer operating at ultraviolet wavelengths and is one of six remote sensing instruments on Solar Orbiter. The mission seeks to understand how the sun creates and controls the heliosphere. SPICE will aid this mission by providing quantitative knowledge of the physical state and composition of the plasmas at the solar source region and by investigating the links between the solar surface, corona and inner heliosphere [1].

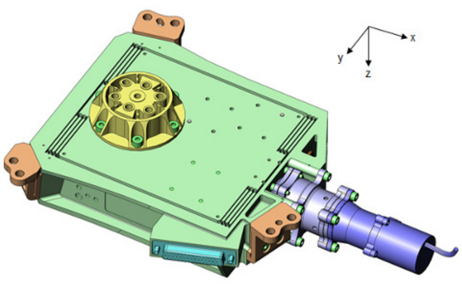

Figure 1. Scan and Focus Mechanism (SFM)

The SFM (Fig. 1) allows for control of the instrument's primary mirror about two degrees of freedom. A linear stage is used to focus the mirror along the optical x-axis relative to an entrance slit. A second stage within this focus stage allows rotational movement about the rotational z-axis, allowing the image of the Sun to be scanned across the slit. During each scan the image is stepped in increments equal to the selected slit width, allowing the region of interest to be completely sampled.

The primary mirror is held within a mount that is fixed to the upper interface of the rotary flexure stage.

2. MECHANISM DESIGN

2.1 Main Requirements

The mechanism is required to continuously scan during three 10-day observation windows per orbit, with a total of up to 160 days of observing over nominal and extended operations. This equates to almost 70,000 end-to-end scan cycles over the full 8 arcmin rotation range (equivalent to 16 arcmin on the solar disk), with nearly 6000 allocated to ground activities before the application of lifetime factors. The minimum slit width is 1 arcsec and the repeatability target is ±0.1 arcsec. These represent increased repeatability and scan range over the EIS instrument on Hinode (formerly Solar B) [2].

Focus adjustment will be performed as required during in-orbit commissioning and between observation windows over a range of up to ±0.5mm with 64 and 32 full cycles allocated to ground and orbital cycles respectively. The required resolution is 1µm or better although adjustment steps will typically be at 5µm intervals.

The mechanism is designed to provide nominal performance between -30°C and +60°C and is required to withstand non-operational temperatures during flight of -60°C to +65°C. The SFM is also subject to the strict contamination requirements of an extreme ultraviolet optical system, which impacts aspects such as lubrication selection and process control. Consistent with previous similar solar missions such as the long-lived SOHO spacecraft [3,4,5], the use of only solid lubricants was specified.

2.2 Mechanism Architecture and Structure

The mechanism design is driven by the need to maintain stability and achieve the required resolution and repeatability whilst observing the packaging constraints of the instrument concept. It is located on the underside

Proc. '16th European Space Mechanisms and Tribology Symposium 2015', Bilbao, Spain, 23–25 September 2015 (ESA SP-737, September 2015)

of the instrument optical bench structure, with the crown of the scan stage protruding up into the optics enclosure. The mirror in its mount is fitted from the enclosure side during integration and sealed using a flexible viton seal. Since the mirror is cantilevered, it is restrained by a pin and snubber at the free end. The proposed concept had made provision for an integral supporting structure for the mirror, but the instrument structure and seal design evolved so as to make this impractical. Various launch lock options were explored, but were deemed unnecessary.

The mechanism is mounted isostatically on three flexural foot supports, centred on the rotational axis. These are sufficiently compliant to allow the structure of the mechanism to expand and contract at a different rate to the underlying optical bench in order to maintain a consistent relative location of the scanning axis under varying thermo-elastic load-cases. The differential expansion is small however, so they are rigid enough to support the structure under high level dynamic loading. The main structural component comprises an outer structural frame which surrounds the focus stage enclosure, suspended on linear flexures in the centre. This contains a scan actuator and sensors for both the scan and focus stages, while a cover offers increased rigidity (Fig. 2). The torsional flexures that allow scan rotation sit within the focus stage with radial flexures that extend through the structure. Within the enclosure a drive arm and a sensor lever arm are fitted on either side.

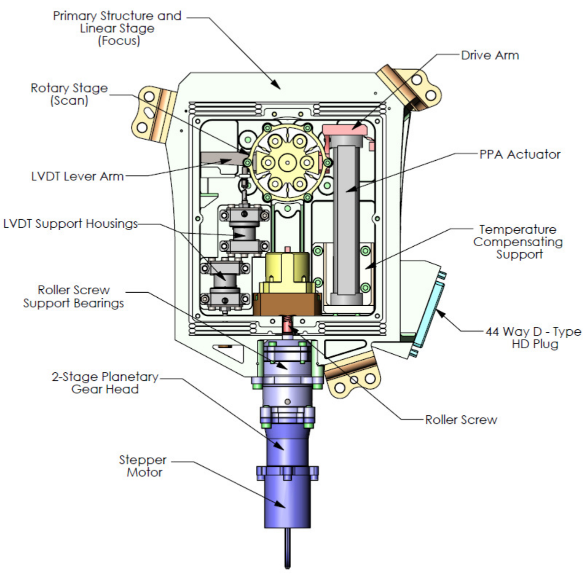

Figure 2. SFM Components

Titanium alloy was used for all of the main structural components as its favourable strength/stiffness ratio ensures that it is suitable for flexure applications, while the CTE is suitably low to be close to that of the optics bench. Building on the heritage of previous flexure-based structural systems, wire electrical discharge machining (WEDM) was used to manufacture the flexure geometry with the process carefully controlled to maximise fatigue life in the flexures. The blade geometry of each stage was optimised to withstand dynamic loading, while minimising the drive force required from each actuator. The symmetry of the flexure arrangement and the monolithic structure of the flexure components (Fig. 3) ensures that cross-coupling between these two degrees of freedom is kept to a minimum and overall structural stability is maintained.

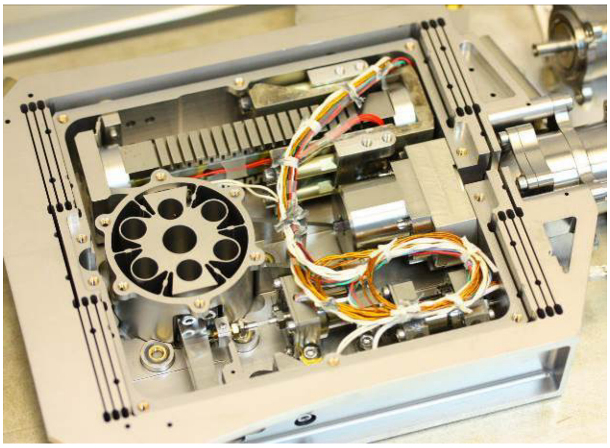

Figure 3. Underside with cover removed

The material selection and geometrical complexity creates a thermally isolated structure. While the environment is typically within the normal temperature range for space hardware, the presence of high flux on the mirror and the predicted temperatures during non-operational phases and qualification testing mean that the temperature limitations of the proposed elements of the mechanism had to be carefully considered.

Each stage is constrained by a drive actuator, which ensures rigidity during launch. These actuators provide the necessary range of motion with sufficient force to achieve the required motorisation margins. In order to simplify the mechanism only one actuator is employed for each degree of freedom and full redundancy is not incorporated. This minimises the overall mass and volume, increasing structural margins and reducing the packaging volume in an already challenging envelope. It also reduces the need for additional complexity to achieve the independence of the two systems, which in itself would introduce further failure modes. This is also in line with the general instrument approach.

2.3 Focus Mechanism

The focus mechanism is driven by a Phytron stepper motor combined with a 49:1 epicyclic (planetary) gearbox. The motor and gearbox bearings are ESTL PVD lead lubricated with lead-bronze cages. The gearbox also uses PVD lead on the gears in combination with a minimal amount of Braycote 601EF grease applied in the gearbox. This was deemed allowable because the mechanism sits entirely outside of the optics unit.

Due to the cantilevered nature of the motor and coupling, an additional flexure-based clamp had to be incorporated to limit the dynamic response during vibration. This was due to the predicted exceedance of the manufacturer's $40g_{rms}$ rating, although there was significant conservatism in the specified levels and assumed damping, particularly early in the programme.

While the intermittent operation of the focus mechanism ensures that thermal performance is not critical, the motor windings are connected in series to reduce power dissipation and increase the limit on the duty cycle of the mechanism. The local temperature limit of the windings during operation is 150ºC and, since this may be reached at high ambient temperatures, any usage constraints are determined during qualification.

Conversion of the rotary stepper motor motion into linear displacement is performed using a Rollvis planetary roller-screw. A roller-screw was selected after a trade-off against other candidate options, one advantage being that they typically offer higher thrust load capacities than either lead or ball screws. However, special care was taken to ensure a compliant preload was applied to compensate for any surface modification of the rigid screw contacts and to make the system less susceptible to the effects of any debris generation or thermal gradients.

The load limitations of the motor bearings required the use of additional support bearings to take the reaction loads from the roller-screw during launch and when driving against the flexures. The type selected for this purpose was Barden 1902H angular contact bearings, made from SAE 52100 bearing steel and hard preloaded in back-to-back configuration. The bearings are ESTL PVD lead lubricated and use a lead-bronze cage. A specially designed compliant shaft coupling is used to limit any load transfer into the motor gearbox bearings.

2.4 Scan Mechanism

The actuator for the scan mechanism is a CEDRAT parallel pre-stressed actuator (PPA). A PPA was selected as their high force density, life-time and potentially high resolution make them suitable for fine scanning applications such as this. Piezo actuators are no longer considered new technology and have been used in a number of high precision instrument mechanisms [6,7,8,9] and CEDRAT PPA actuators have undergone general qualification for the 5x5x20 line of components [10].

The force generated by the PPA is roughly proportional to the applied voltage, which in this case is between 5 and 150V. The scan mechanism is driven by the linear actuator at a radius of around 25mm via a drive arm. As the actuator is unable to sustain significant torsional loading or bending moments, the drive arm is designed with a controlled compliance to ensure that moment loads are eliminated. The achievable stroke is dependent on the stiffness ratio of the actuator and the driven load – it generates maximum force when driven against a rigid load or, conversely, achieves maximum stroke when driven unloaded. In the case of this mechanism, the compliance of the scan flexure is kept to approximately 10% of that quoted for the actuator, ensuring that the stroke is kept close to that achievable in an unconstrained configuration.

Whilst the majority of the structure is Titanium, the PPA has a significantly lower CTE. Thermally compensating structure is incorporated to minimise rotation of the scan mirror with temperature. This was designed to be tuneable as this behaviour was better characterised during the course of the programme. With such a small scanning range it is necessary to minimise such errors as far as possible. In this case the target was to ensure that a consistent 8 arcmin scanning range could be achieved at all temperatures given the variations in pointing and PPA stroke with temperature.

The main temperature limitation on the piezo actuator is that the ceramic elements should remain below their curie temperature of around 150ºC to avoid depolarization. As this is the case, an environmental temperature limit of 100ºC has been implemented for this component. The static operation of the actuator means that the power dissipation within the device is likely to be very low, although the thermal conductivity of such devices is very poor. There are also restrictions due to humidity, as such devices can be damaged by operation in higher humidity environments. While it is not expected that the PPA will be operated at such levels, any operation above 60% RH will be recorded as this is the highest level for which lot acceptance testing was performed. Since our cleanroom environment may be up to 65% RH, any operation between these two levels will be monitored. However, the humidity has historically tended to be at the lower end of the required range.

2.5 Position Sensing

The successful operation of both of the mechanisms, but particularly the scan function which operates in closed loop, is dependent on maximising the resolution of the position feedback. Each stage has a linear variable differential transducer (LVDT), and in both cases the Measurement Specialities (formerly Schaevitz) MHR 025 was selected. These are operated in unipolar mode to avoid the impact of zero crossings which were found to be problematic during testing on early models.

Each LVDT body is clamped rigidly in its own housing while flat chemically etched springs clamped at either end of the LVDT housing provide support for the LVDT core and push-rod. Bread-boarding activities initially used guide bushes, but it was clear that any friction in the system would introduce hysteresis into the position measurement and so a fully elastic, frictionless support was required. The flat springs support the pushrod in plane whilst still allowing free axial movement required for measurement (Fig. 4).

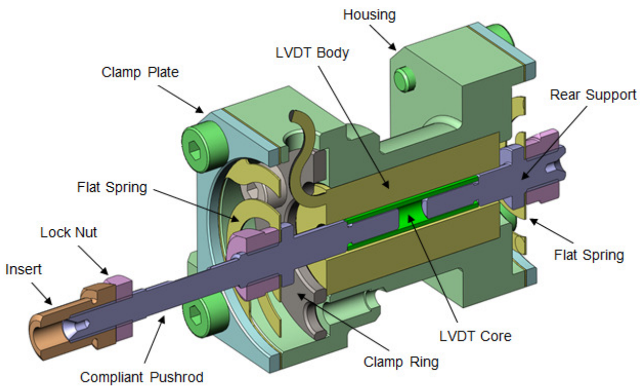

Figure 4. LVDT subassembly

The focus LVDT is connected directly to the static structure to sense the relative motion over its stroke of ±0.5mm. For the scan mechanism a mechanical pivoting arm is used to amplify the small displacements from the scan stage to maximise the high resolution required for the scanning function. The amplifying arm converts the small displacement at the end of the lever arm on the scan flexure into a linear movement of the push-rod close to the total linear range of the LVDT, thus maximising sensitivity. The scan pushrod incorporates a flexure, to take out any rotational motion and transfer of radial forces to the LVDT assembly, maintaining concentricity of the core within the LVDT body.

3. DEVELOPMENT CHALLENGES

3.1 General Approach

A proactive approach was taken to address areas of uncertainty and where development risks had been identified. Experience from previous programmes had highlighted the importance of gaining early experience of unfamiliar or novel elements of the system, which is important when embarking on an entirely new concept.

A cautious model philosophy was taken with rapid progress made on bread-boarding activities from the outset. Early in the programme an additional model was introduced in order to decouple unit level qualification activities from customer deliverable hardware. In hindsight this was a good decision as the opportunity to implement corrective action in the qualification and flight models is highly valuable, not to mention costly and disruptive if discovered later in the programme.

3.2 PPA Implementation and Operation

One key area of the design process was ensuring that the challenging scan mechanism performance requirements could be achieved. This requires maximising the available stroke, whilst ensuring that adequate margin is available to cover thermal and drift effects. There are also aspects that are difficult to fully characterise such as thermal expansion coefficient, force variation with temperature and drift effects. These are dependent on a range of factors specific to the application and environment and, for this reason, initial measurements were at times misleading due to critical differences in the setup compared with the final application.

There were also issues related to this actuator, which has a greater cross-sectional area than those qualified previously. As such, CEDRAT have refined the soldering process to avoid propagation of micro-cracks within the ceramic which were identified during destructive parts analysis.

Correction of the differential CTE between the PPA and the underlying titanium structure was one area that has required careful consideration. Due to the change in force capability with temperature (approximately 0.3% per °C), the coverage of the angular range at the minimum qualification has little margin. As such, any CTE correction had to ensure good image overlap over the temperature range. Since the scanning is performed from one end of the range, it was best to slightly under-correct the CTE when at 0V to get proper overlap over the range 5-150V. This means that, for a perfect linear actuator with no hysteresis or drift, the pointing should essentially be invariant with temperature at target voltage of 77.5V rather than remaining constant at 0V.

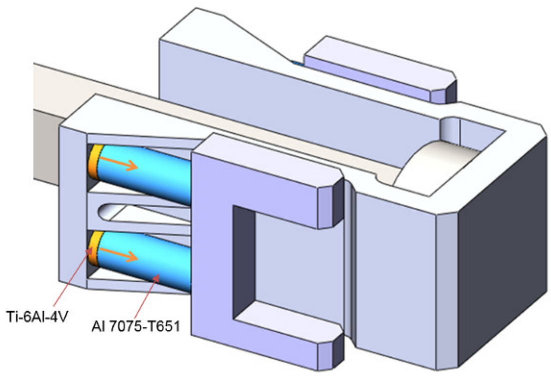

Figure 5. Thermo-elastic compensation

In order to achieve this CTE correction the PPA was mounted in a thermal compensation support (Fig. 5). The main structure of the support was manufactured from Invar due to its low CTE. The system also made use of aluminium and titanium spacers which allowed the thermal performance of the system to be tuned by adjusting spacer length.

Fig. 6 shows the predicted image position, plotted to scale, which demonstrates the variation between image positions at different temperatures. The decision was made to remain close to the left hand image alignment, to ensure that variation in temperature does not result in excessive stresses being induced in the flexures. The endurance limit of the flexures is reached once the mirror rotation exceeds approximately 8.7 arc minutes, so there are restrictions on voltage at higher temperatures that should be observed.

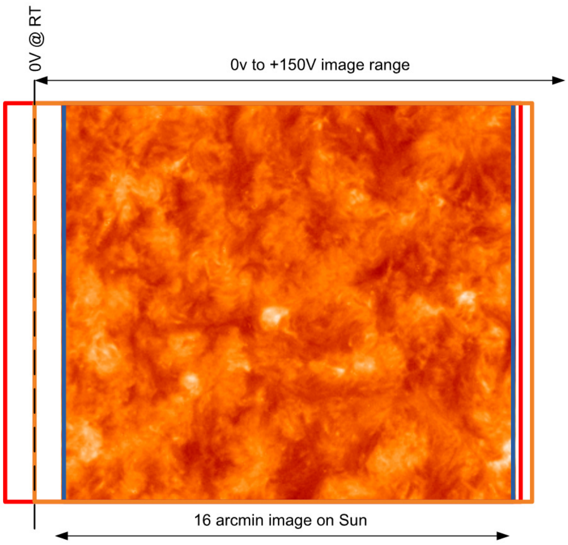

Figure 6. Scan range overlap at cold, ambient and hot

There is also a slight skew in the image due to parasitic rotation in the scan flexure. The mirror nods slightly as it is rotated by approximately 10 arcsec, but this has been measured in line with prediction and is well within the requirement.

3.3 Flexure Fatigue

Fatigue failure of flexures is a concern given the criticality of these to the mechanism function. This was borne in mind during the design phase, with all flexure stresses kept below the endurance limit of the material. In this case a conservative value of 350 MPa for wire-cut titanium was used, that is based on proprietary test data from another programme and has historically been assumed for all of our flexure designs. However concerns about alpha case in light of recent failures on other programmes meant that further validation of these assumptions was required.

The alpha case is a brittle surface layer that can act as a failure initiation area and in turn impact fatigue life. In order to maximise performance, it should ideally be removed. While this is well known to form at the surface during wire-cutting operations, the nature of the layer is dependent on the cutting parameters. These parameters were investigated in a process validation activity to study the alpha-case and recast layers, methods of removal and influence on fatigue life.

Two main areas were identified for investigation. The first was related to increasing the number of cutting passes completed during manufacture. Previous research [11] demonstrated a reduction in recast layer thickness as the number of wire cutting passes is increased. The second aspect was identifying and qualifying a chemical descaling process to remove any layer that remained after machining. In order to investigate these two processes, test samples matching the geometry of the focus stage flexures were manufactured using a Charmilles 300 clean cut wire machine. Some of the samples also underwent an acid descaling process based on the requirements specified in [12] and [13].

The investigation concluded that there was a significant amount of recast layer generated on the surface of the test pieces that had undergone one or two passes. In the areas that had received four or five passes, however, the level of recast layer generated was reduced to a thickness of approximately two microns. In addition, expected improvements in surface roughness and blade thickness tolerances were verified. Fig. 7 displays two samples, one that had undergone one wire cutting pass (left image) and one that received four passes (right image).

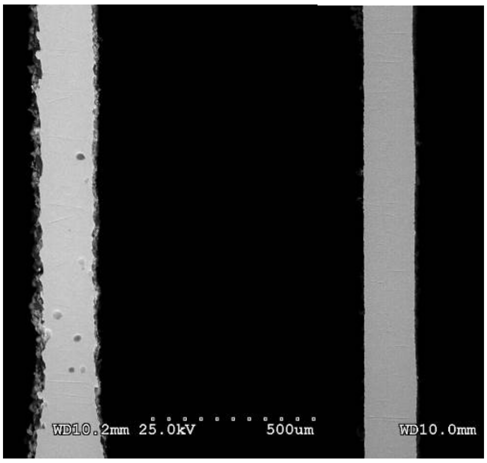

Figure 7. Flexure cross-sections

The investigation also demonstrated that the acid descaling process selected was suitable for removing the layer. Due to the nature of the acid descaling process there is also increased potential for Hydrogen embrittlement. The approach taken for this mechanism combined a high number of wire cutting passes with a shorter bath duration to remove the layer with minimum impact on the thickness tolerances.

In order to validate this approach a series of fatigue tests were carried out on the samples. The results demonstrated that the combination of completing a high number of passes on the clean cut machine and carrying out a chemical descaling process produced a higher level of fatigue performance than previously assumed for this application. These results suggest an endurance limit closer to that expected from conventionally machined material although the descaling operation did not appear to be critical in this respect.

3.4 Roller-screw Configuration

There are very few examples of dry lubricated roller-screws in space instrument applications and many potential pitfalls. The most relevant available heritage comes from the SUMER instrument on SOHO [3,4] but the lack of a dry nitrogen purge for ground operations forced us to look at lead lubrication heritage rather than MoS_2. While there is little clear precedent, we were able to implement a number of lessons learned resulting in a configuration that we were confident would achieve the relatively low number of cycles required.

Aspects such as preload compliance, materials and running in procedures were considered carefully. A confidence test was subsequently performed as a precursor to the life-test to highlight any potential issues with the lubrication and characterise the torque performance and efficiency of the roller-screw assembly. The test items were flight representative components from the SFM focus actuation system including the stepper motor, support bearings and roller-screw. The test rig used wave springs to provide a representative resistance similar to the focus stage in terms of axial stiffness. The assembly was mounted to a Kistler load and torque transducer to provide both torque and axial force measurements.

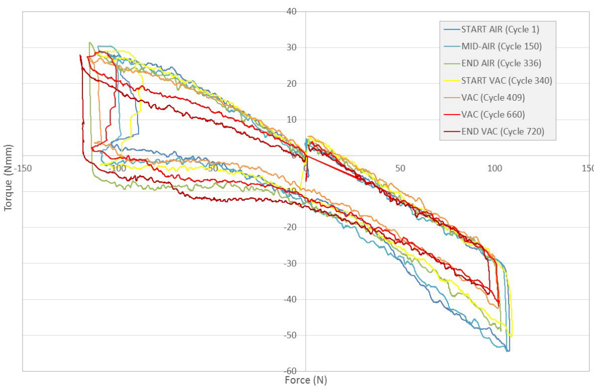

Figure 7. Roller-screw test data

After an initial running-in process, performed under vacuum with the external loading removed, a long term running phase was then completed with 336 cycles completed in air followed by 384 cycles in vacuum. The number of cycles selected was equivalent to those required during the mechanism life test. Torque vs. axial force is plotted in Fig. 7. The plots illustrate the characteristics of the roller-screw which is dependent on the direction of travel due to the preloading configuration, although there is some drift in the measurements. Over the course of the 720 cycles, the torque change due to change of direction (right hand side) can be seen to decrease as the test progresses. This may be interpreted as the roller-screw continuing to fully run-in over the course of the life-test.

As the roller-screw performed well during the test, it was possible to proceed to qualification testing with increased confidence in the system.

3.5 Motor Lubrication

As with the roller-screws, the use of MoS2 was deemed impractical due to the need for several hundred operations in air after the application of life-test factors and an additional allocation for cycles prior to delivery. While the use of lead is a good choice for bearing applications, it is less well suited to the lubrication of sliding contacts. While the relatively benign life requirements have not posed a problem for the rotary bearings, roller-screw or gear teeth, it was the planetary gear plain bearings that were found to be problematic with this regime.

It was intended to introduce self-lubricating planet gear bushes in the gearbox, but there was some reluctance by the supplier to perform this modification. It was confirmed during testing that the performance of lead at this interface was likely to degrade, thus impacting the efficiency of the gear train in the gearhead. In agreement with the customer, and after some effort to justify its use, it was decided to implement our back-up option and introduce a small amount of the Braycote 601EF grease lubrication into the gearbox. This required the introduction of additional sealing components to minimise evaporation and loss of oil into the local environment. A detailed evaporation and seal analysis was performed to support this decision. While EUV instruments are highly sensitive to contamination of this type, the strict requirement prohibiting liquid lubricants was challenged due to the location of the mechanism being remote from the optics enclosure and its apertures. In addition the minimal quantities used, application of creep barrier and seal design reduce the overall loss of oil to exceptionally low levels over the mission life.

It was apparent during this process that there is little data for the estimation of the efficiency of multi-stage gearboxes and, in the case of grease lubrication, the impact of temperature. The propagation of errors in the efficiency estimation or friction variability in each stage makes the system particularly sensitive with respect to motorisation.

3.6 Hyperstatic/Integration Stresses

One aspect of the design of such structures is the introduction of stresses during integration. While the monolithic components may be relatively free of residual stresses, care has to be taken with those components that are assembled into the system to ensure that excessive stresses do not arise as a result of being over constrained during assembly. For relatively stiff flexures, such stresses can easily be introduced inadvertently.

While these were analysed for the major structural parts during detailed analysis, there were instances where these were not carefully considered as they should have been. Such stresses introduced as the result of assembly tolerances or locked in torques from assembly operations can easily introduce stresses which risk damage once dynamic loading is applied. Sensitive components are most at risk since they can easily be stressed as the result of fastening operations, which are high compared to the loads expected during vibration.

4. QUALIFICATION AND LIFE-TESTING

4.1 Test Facility

Qualification testing of the mechanism is being performed within the test facility shown below in Fig. 8.

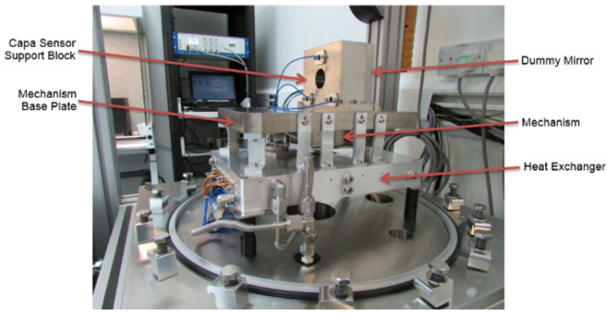

Figure 8. Thermal Vacuum Test Rig

The primary method of verifying mechanism performance was through the use of a titanium dummy mirror mounted to the scan stage via a titanium mirror mount. The dummy mirror acts as a target for a set of three capacitive sensors and a ¼ wave plane mirror is also mounted on its surface to allow theodolite measurements to be made. The capacitive sensors were supplied by Micro-Epsilon and have a resolution of 1.5nm and a measuring range of 2mm. In order to remove any thermal effects the capacitive sensors are mounted within an invar block. The mechanism is mounted to a separate invar base plate which provides high dimensional stability with a CTE close to that of the optics bench.

Due to the strict cleanliness levels a dry pumping system was selected. The chamber can also be equipped with an RGA to permit cleanliness to be assessed prior to test item installation.

4.2 Qualification Testing

Qualification testing started with a number of ground cycles of the mechanism before thermal and structural testing. The mechanism has proven to be highly stable during thermal cycling with parasitic displacements and rotations close to prediction. The mirror rotation has been well characterised, though achieved using inputs from the test EGSE rather than a representative drive unit, which is being developed in the US by SwRI. The performance of the mechanism at system level has been reported as being within specification.

Shock testing was completed successfully, but it was in the subsequent vibration test that problems were encountered. A failure in the LVDT support springs, which subseqently propagated into some of the surrounding components halted the test and have taken a number of months to correct. This has been attributed to the aforementioned problem of hyperstatism in the failed components, which were almost certainly stressed before the commencement of the test. This has been addressed by the modification of the design of these components, the introduction of a snubber to limit the torsional mode of the mirror and a number of process changes. The re-designed springs are also paired in order to provide a level of redundancy.

5. LESSONS LEARNED

A number of lessons were learned during the course of this programme, including:

- Motorisation calculations involving complex transmission chains are not be straightforward. In particular the propagation of efficiency estimation errors in multi-stage transmissions can result in considerable errors in system level predictions.
- When using PPA actuators for positioning applications, the nominal usable stroke will be significantly reduced due to hysteresis, drift and thermal effects as well as other environmental, electrical and mechanical influences. For example, the CTE is dependent on the electrical connections (also see [7]).
- Ensure that hyperstatic load-cases are

comprehensively assessed. This is arguably more important for small localised components as it is for major structural components.

- Early testing to target specific risks gives confidence as well as highlighting potential issues. However, these are almost always limited in how representative they can be.
- The use of snubbers, while sometimes seen as a solution to certain structural problems, tends to introduce large uncertainties into modelling. It can also introduce problems with control during dynamic testing. A robust design avoiding structural non-linearities from the outset is almost always preferable.

6. CONCLUSIONS

At the time of writing, the qualification of the mechanism is nearing completion with the FM builds about to commence.

7. ACKNOWLEDGEMENTS

The authors would like to acknowledge the support and cooperation of all the industrial partners on the programme, in particular Paul Eccleston and Doug Griffin from RAL Space, the instrument prime contractor, who have demonstrated their expertise in the development of science instrumentation throughout this programme. We also gratefully acknowledge the support of Ronan Le Letty and Anne Pacros, ESA ESTEC, who have overseen the instrument and mechanisms development with great professionalism.

8. REFERENCES

1. Fludra, A. et al. (2013). SPICE EUV Spectrometer for the Solar Orbiter Mission. '*Proc. SPIE 8862, Solar Physics and Space Weather Instrumentation V, 88620F'*. San Diego, California, United States.

2. Korendyke, C.M. et al. (2006). Optics and Mechanisms for the Extreme-Ultraviolet Imaging Spectrometer on the Solar-B Satellite. *Appl. Opt.* 45, 8674-8688

3. Engelhardt, W. & Hartwig, H. (1992). Ultra-Clean High-Precision Mechanisms for the SUMER EUV Spectrometer on SOHO. In '*Proc. 5th European Space Mechanisms and Tribology Symposium, Noordwijk'*, ESA SP-334, Noordwijk, The Netherlands, pp79-82.

4. Hartwig, H. et al. (1995). Mechanism Qualification for SOHO SUMER, Results and Lessons Learned. In '*Proc. 6th European Space Mechanisms and Tribology Symposium, Zurich'*, ESA SP-374, Noordwijk, The Netherlands, pp383-384.

5. Sawyer, E. & Long, J. (2001). A Review of the Mechanisms on SOHO/CDS After Five Years in Orbit. In '*Proc. 9th European Space Mechanisms and Tribology Symposium, Liege'*, ESA SP-480, Noordwijk, The Netherlands, pp107-111.

6. Burger, F. & Eder, J. (1995). High Precision Pointing Device for the LASCO Instrument on SOHO. In '*Proc. 6th European Space Mechanisms and Tribology Symposium, Zurich'*, ESA SP-374, Noordwijk, The Netherlands, pp9-14.

7. Le Letty, R. et al. (2001). The Scanning Mechanism for Rosetta/MIDAS From an Engineering Model to the Flight Model. In '*Proc. 9th European Space Mechanisms and Tribology Symposium, Liege'*, ESA SP-480, Noordwijk, The Netherlands.

8. Le Letty, R. et al. (2007). The Design and Qualification of the Piezo Actuated Optical Delay Line for Lisa-Pathfinder-LTP. In '*Proc. 12th European Space Mechanisms and Tribology Symposium, Liverpool'*, ESA SP-653, Noordwijk, The Netherlands.

9. Barillot, F. & Bourgain, F. (2015, March 12th). *ATLID Beam Steering Mirror.* [Presentation Slides]. Presented at ESA Mechanisms Final Presentation Days, ESTEC.

10. Barillot, F. & Bourgain, F. (2015, March 12th). *Piezo Actuator Qualification.* [Presentation Slides]. Presented at ESA Mechanisms Final Presentation Days, ESTEC.

11. Antar, M.T. et al. (2010). WEDM of Aerospace Alloys Using 'Clean Cut' Generator Technology. In '*Proc. 16th International Symposium on Electromachining (ISEM)'*, Shanghai Jiao Tong University Press, pp285-290.

12. ASTM International. (2006). *B600-91 (2002)$^{\epsilon 1}$, Standard Guide for Descaling and Cleaning Titanium and Titanium Alloy Surfaces.* West Conshohocken, PA.

13. NASA, Engineering Directorate, Structural Engineering Division (2007). NASA PRC-5010C, Process Specification for Pickling, Etching, and Descaling of Metals. Lyndon B. Johnson Space Centre, Houston, TX.